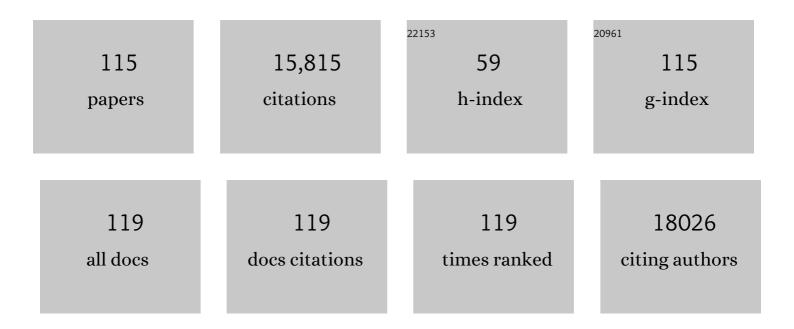
## Yang Huang

List of Publications by Year in descending order

Source: https://exaly.com/author-pdf/28907/publications.pdf Version: 2024-02-01



#	Article	IF	CITATIONS
1	Boron Nitride Nanotubes and Nanosheets. ACS Nano, 2010, 4, 2979-2993.	14.6	1,981
2	An extremely safe and wearable solid-state zinc ion battery based on a hierarchical structured polymer electrolyte. Energy and Environmental Science, 2018, 11, 941-951.	30.8	731
3	Photoluminescent Ti <sub>3</sub> C <sub>2</sub> MXene Quantum Dots for Multicolor Cellular Imaging. Advanced Materials, 2017, 29, 1604847.	21.0	692
4	A self-healable and highly stretchable supercapacitor based on a dual crosslinked polyelectrolyte. Nature Communications, 2015, 6, 10310.	12.8	634
5	Nanostructured Polypyrrole as a flexible electrode material of supercapacitor. Nano Energy, 2016, 22, 422-438.	16.0	629
6	Highly Flexible, Freestanding Supercapacitor Electrode with Enhanced Performance Obtained by Hybridizing Polypyrrole Chains with MXene. Advanced Energy Materials, 2016, 6, 1600969.	19.5	580
7	Voltage issue of aqueous rechargeable metal-ion batteries. Chemical Society Reviews, 2020, 49, 180-232.	38.1	522
8	An Intrinsically Stretchable and Compressible Supercapacitor Containing a Polyacrylamide Hydrogel Electrolyte. Angewandte Chemie - International Edition, 2017, 56, 9141-9145.	13.8	458
9	Texturing in situ: N,S-enriched hierarchically porous carbon as a highly active reversible oxygen electrocatalyst. Energy and Environmental Science, 2017, 10, 742-749.	30.8	451
10	Waterproof and Tailorable Elastic Rechargeable Yarn Zinc Ion Batteries by a Cross-Linked Polyacrylamide Electrolyte. ACS Nano, 2018, 12, 3140-3148.	14.6	439
11	Multifunctional Energy Storage and Conversion Devices. Advanced Materials, 2016, 28, 8344-8364.	21.0	420
12	From Industrially Weavable and Knittable Highly Conductive Yarns to Large Wearable Energy Storage Textiles. ACS Nano, 2015, 9, 4766-4775.	14.6	411
13	High-performance stretchable yarn supercapacitor based on PPy@CNTs@urethane elastic fiber core spun yarn. Nano Energy, 2016, 27, 230-237.	16.0	297
14	Magnetic-Assisted, Self-Healable, Yarn-Based Supercapacitor. ACS Nano, 2015, 9, 6242-6251.	14.6	291
15	Polyurethane/Cotton/Carbon Nanotubes Core-Spun Yarn as High Reliability Stretchable Strain Sensor for Human Motion Detection. ACS Applied Materials & Interfaces, 2016, 8, 24837-24843.	8.0	251
16	Super-high rate stretchable polypyrrole-based supercapacitors with excellent cycling stability. Nano Energy, 2015, 11, 518-525.	16.0	248
17	Porous Fe3O4/carbon composite electrode material prepared from metal-organic framework template and effect of temperature on its capacitance. Nano Energy, 2014, 8, 133-140.	16.0	232
18	Towards wearable electronic devices: A quasi-solid-state aqueous lithium-ion battery with outstanding stability, flexibility, safety and breathability. Nano Energy, 2018, 44, 164-173.	16.0	228

#	Article	IF	CITATIONS
19	Mn <sub>3</sub> O <sub>4</sub> nanoparticles on layer-structured Ti <sub>3</sub> C <sub>2</sub> MXene towards the oxygen reduction reaction and zinc–air batteries. Journal of Materials Chemistry A, 2017, 5, 20818-20823.	10.3	226
20	Biochar modification significantly promotes the activity of Co3O4 towards heterogeneous activation of peroxymonosulfate. Chemical Engineering Journal, 2018, 354, 856-865.	12.7	212
21	Activated boron nitride as an effective adsorbent for metal ions and organic pollutants. Scientific Reports, 2013, 3, 3208.	3.3	203
22	Synthetic Routes and Formation Mechanisms of Spherical Boron Nitride Nanoparticles. Advanced Functional Materials, 2008, 18, 3653-3661.	14.9	196
23	Proton-Insertion-Enhanced Pseudocapacitance Based on the Assembly Structure of Tungsten Oxide. ACS Applied Materials & Interfaces, 2014, 6, 18901-18910.	8.0	182
24	Boosting the Yield of MXene 2D Sheets via a Facile Hydrothermal-Assisted Intercalation. ACS Applied Materials & Interfaces, 2019, 11, 8443-8452.	8.0	178
25	A Highly Durable, Transferable, and Substrateâ€Versatile Highâ€Performance Allâ€Polymer Microâ€Supercapacitor with Plugâ€andâ€Play Function. Advanced Materials, 2017, 29, 1605137.	21.0	160
26	Self-Standing Polypyrrole/Black Phosphorus Laminated Film: Promising Electrode for Flexible Supercapacitor with Enhanced Capacitance and Cycling Stability. ACS Applied Materials & Interfaces, 2018, 10, 3538-3548.	8.0	159
27	Inâ€Situ Electrochemically Activated Surface Vanadium Valence in V <sub>2</sub> C MXene to Achieve High Capacity and Superior Rate Performance for Znâ€Ion Batteries. Advanced Functional Materials, 2021, 31, 2008033.	14.9	156
28	Polymer composites of boron nitride nanotubes and nanosheets. Journal of Materials Chemistry C, 2014, 2, 10049-10061.	5.5	153
29	Efficient heterogeneous activation of peroxymonosulfate by facilely prepared Co/Fe bimetallic oxides: Kinetics and mechanism. Chemical Engineering Journal, 2018, 345, 364-374.	12.7	151
30	Nanoscale Parallel Circuitry Based on Interpenetrating Conductive Assembly for Flexible and Highâ€Power Zinc Ion Battery. Advanced Functional Materials, 2019, 29, 1901336.	14.9	145
31	Component Matters: Paving the Roadmap toward Enhanced Electrocatalytic Performance of Graphitic C <sub>3</sub> N <sub>4</sub> -Based Catalysts <i>via</i> Atomic Tuning. ACS Nano, 2017, 11, 6004-6014.	14.6	144
32	Facile Processing of Free-Standing Polyaniline/SWCNT Film as an Integrated Electrode for Flexible Supercapacitor Application. ACS Applied Materials & amp; Interfaces, 2017, 9, 33791-33801.	8.0	139
33	Thickness-dependent bending modulus of hexagonal boron nitride nanosheets. Nanotechnology, 2009, 20, 385707.	2.6	134
34	A shape memory supercapacitor and its application in smart energy storage textiles. Journal of Materials Chemistry A, 2016, 4, 1290-1297.	10.3	134
35	Capacitance Enhancement in a Semiconductor Nanostructureâ€Based Supercapacitor by Solar Light and a Selfâ€Powered Supercapacitor–Photodetector System. Advanced Functional Materials, 2016, 26, 4481-4490.	14.9	133
36	An electrochromic supercapacitor and its hybrid derivatives: quantifiably determining their electrical energy storage by an optical measurement. Journal of Materials Chemistry A, 2015, 3, 21321-21327.	10.3	124

#	Article	IF	CITATIONS
37	Leadâ€Free Perovskite Derivative Cs <sub>2</sub> SnCl <sub>6â°'</sub> <i><sub>x</sub></i> Br <i><sub>x</sub></i> Single Crystals for Narrowband Photodetectors. Advanced Optical Materials, 2019, 7, 1900139.	7.3	123
38	Chemical activation of boron nitride fibers for improved cationic dye removal performance. Journal of Materials Chemistry A, 2015, 3, 8185-8193.	10.3	121
39	A high performance fiber-shaped PEDOT@MnO <sub>2</sub> //C@Fe <sub>3</sub> O <sub>4</sub> asymmetric supercapacitor for wearable electronics. Journal of Materials Chemistry A, 2016, 4, 14877-14883.	10.3	118
40	Ultrathin h-BN/Bi2MoO6 heterojunction with synergetic effect for visible-light photocatalytic tetracycline degradation. Journal of Colloid and Interface Science, 2021, 589, 545-555.	9.4	115
41	Toward enhanced activity of a graphitic carbon nitride-based electrocatalyst in oxygen reduction and hydrogen evolution reactions via atomic sulfur doping. Journal of Materials Chemistry A, 2016, 4, 12205-12211.	10.3	112
42	Solvothermal Synthesis of Ultrathin Cesium Lead Halide Perovskite Nanoplatelets with Tunable Lateral Sizes and Their Reversible Transformation into Cs <sub>4</sub> PbBr <sub>6</sub> Nanocrystals. Chemistry of Materials, 2018, 30, 3714-3721.	6.7	108
43	3D spacer fabric based multifunctional triboelectric nanogenerator with great feasibility for mechanized large-scale production. Nano Energy, 2016, 27, 439-446.	16.0	107
44	Extremely Stable Polypyrrole Achieved via Molecular Ordering for Highly Flexible Supercapacitors. ACS Applied Materials & Interfaces, 2016, 8, 2435-2440.	8.0	99
45	Architecting Amorphous Vanadium Oxide/MXene Nanohybrid via Tunable Anodic Oxidation for Highâ€Performance Sodiumâ€ion Batteries. Advanced Energy Materials, 2021, 11, 2100757.	19.5	99
46	Bulk synthesis, growth mechanism and properties of highly pure ultrafine boron nitride nanotubes with diameters of sub-10 nm. Nanotechnology, 2011, 22, 145602.	2.6	97
47	Light-permeable, photoluminescent microbatteries embedded in the color filter of a screen. Energy and Environmental Science, 2018, 11, 2414-2422.	30.8	97
48	Conjugated System of PEDOT:PSS-Induced Self-Doped PANI for Flexible Zinc-Ion Batteries with Enhanced Capacity and Cyclability. ACS Applied Materials & Interfaces, 2019, 11, 30943-30952.	8.0	89
49	Degradation of antibiotics in multi-component systems with novel ternary AgBr/Ag3PO4@natural hematite heterojunction photocatalyst under simulated solar light. Journal of Hazardous Materials, 2019, 371, 566-575.	12.4	87
50	Ultrafine porous boron nitride nanofibers synthesized via a freeze-drying and pyrolysis process and their adsorption properties. RSC Advances, 2016, 6, 1253-1259.	3.6	84
51	Selective adsorption behavior/mechanism of antibiotic contaminants on novel boron nitride bundles. Journal of Hazardous Materials, 2019, 364, 654-662.	12.4	84
52	Highly Integrated Supercapacitorâ€5ensor Systems via Material and Geometry Design. Small, 2016, 12, 3393-3399.	10.0	78
53	Sulfonic-Group-Grafted Ti <sub>3</sub> C <sub>2</sub> T <sub><i>x</i></sub> MXene: A Silver Bullet to Settle the Instability of Polyaniline toward High-Performance Zn-Ion Batteries. ACS Nano, 2021, 15, 9065-9075.	14.6	78
54	Dramatically improved energy conversion and storage efficiencies by simultaneously enhancing charge transfer and creating active sites in MnO x /TiO 2 nanotube composite electrodes. Nano Energy, 2016, 20, 254-263.	16.0	77

#	Article	lF	CITATIONS
55	Fabrication of Boron Nitride Nanosheets by Exfoliation. Chemical Record, 2016, 16, 1204-1215.	5.8	74
56	Hydrothermal synthesis of blue-fluorescent monolayer BN and BCNO quantum dots for bio-imaging probes. RSC Advances, 2016, 6, 79090-79094.	3.6	66
57	Enhanced Tolerance to Stretch-Induced Performance Degradation of Stretchable MnO <sub>2</sub> -Based Supercapacitors. ACS Applied Materials & Interfaces, 2015, 7, 2569-2574.	8.0	65
58	Self-Assembly of Porous Boron Nitride Microfibers into Ultralight Multifunctional Foams of Large Sizes. ACS Applied Materials & Interfaces, 2017, 9, 44732-44739.	8.0	64
59	Facile synthesis of α-Fe <sub>2</sub> O <sub>3</sub> nanodisk with superior photocatalytic performance and mechanism insight. Science and Technology of Advanced Materials, 2015, 16, 014801.	6.1	63
60	An Intrinsically Stretchable and Compressible Supercapacitor Containing a Polyacrylamide Hydrogel Electrolyte. Angewandte Chemie, 2017, 129, 9269-9273.	2.0	58
61	Phosphorusâ€Modulationâ€Triggered Surface Disorder in Titanium Dioxide Nanocrystals Enables Exceptional Sodiumâ€Storage Performance. Angewandte Chemie - International Edition, 2019, 58, 4022-4026.	13.8	56
62	A modularization approach for linear-shaped functional supercapacitors. Journal of Materials Chemistry A, 2016, 4, 4580-4586.	10.3	50
63	Hierarchical Porous RGO/PEDOT/PANI Hybrid for Planar/Linear Supercapacitor with Outstanding Flexibility and Stability. Nano-Micro Letters, 2020, 12, 17.	27.0	50
64	BNnanotubes coated with uniformly distributed Fe <sub>3</sub> O <sub>4</sub> nanoparticles: novel magneto-operable nanocomposites. Journal of Materials Chemistry, 2010, 20, 1007-1011.	6.7	44
65	Robust reduced graphene oxide paper fabricated with a household non-stick frying pan: a large-area freestanding flexible substrate for supercapacitors. RSC Advances, 2015, 5, 33981-33989.	3.6	43
66	Flexible MXene films for batteries and beyond. , 2022, 4, 598-620.		42
67	Significance of B-site cobalt on bisphenol A degradation by MOFs-templated CoxFe3â^'xO4 catalysts and its severe attenuation by excessive cobalt-rich phase. Chemical Engineering Journal, 2019, 359, 552-563.	12.7	41
68	Novel multifunctional cheese-like 3D carbon-BN as a highly efficient adsorbent for water purification. Scientific Reports, 2018, 8, 1104.	3.3	39
69	In Situ Growth of MAPbBr <sub>3</sub> Nanocrystals on Few‣ayer MXene Nanosheets with Efficient Energy Transfer. Small, 2020, 16, e1905896.	10.0	38
70	Facet-Controlling Agents Free Synthesis of Hematite Crystals with High-Index Planes: Excellent Photodegradation Performance and Mechanism Insight. ACS Applied Materials & Interfaces, 2016, 8, 142-151.	8.0	37
71	Strategies Toward Stable Nonaqueous Alkali Metal–O <sub>2</sub> Batteries. Advanced Energy Materials, 2019, 9, 1900464.	19.5	35
72	Battery-Everywhere Design Based on a Cathodeless Configuration with High Sustainability and Energy Density. ACS Energy Letters, 2021, 6, 1859-1868.	17.4	35

#	Article	IF	CITATIONS
73	The Emerging Electrochemical Activation Tactic for Aqueous Energy Storage: Fundamentals, Applications, and Future. Advanced Functional Materials, 2022, 32, .	14.9	34
74	Pairing of Luminescent Switch with Electrochromism for Quasi-Solid-State Dual-Function Smart Windows. ACS Applied Materials & Interfaces, 2018, 10, 31697-31703.	8.0	32
75	A MXene of type Ti3C2Tx functionalized with copper nanoclusters for the fluorometric determination of glutathione. Mikrochimica Acta, 2020, 187, 38.	5.0	32
76	High Capacitive Antimonene/CNT/PANI Freeâ€Standing Electrodes for Flexible Supercapacitor Engaged with Selfâ€Healing Function. Small, 2022, 18, .	10.0	31
77	In Situ Cu-Loaded Porous Boron Nitride Nanofiber as an Efficient Adsorbent for CO <sub>2</sub> Capture. ACS Sustainable Chemistry and Engineering, 2020, 8, 7454-7462.	6.7	30
78	Toward <scp>highâ€performance lithiumâ€oxygen</scp> batteries with cobaltâ€based transition metal oxide catalysts: Advanced strategies and mechanical insights. InformaÄnÃ-Materiály, 2022, 4, .	17.3	29
79	A Wearable Supercapacitor Engaged with Gold Leaf Gilding Cloth Toward Enhanced Practicability. ACS Applied Materials & Interfaces, 2018, 10, 21297-21305.	8.0	28
80	Synthesis of ultra $\hat{a} \in $ stable copper nanoclusters and their potential application as a reversible thermometer. Dalton Transactions, 2017, 46, 14251-14255.	3.3	27
81	Bimetallic AuPd Nanoparticles Loaded on Amine-Functionalized Porous Boron Nitride Nanofibers for Catalytic Dehydrogenation of Formic Acid. ACS Applied Nano Materials, 2021, 4, 1849-1857.	5.0	27
82	High performance UV light photodetectors based on Sn-nanodot-embedded SnO <sub>2</sub> nanobelts. Journal of Materials Chemistry C, 2015, 3, 5253-5258.	5.5	26
83	Desulfurization of Model Oil by Selective Adsorption over Porous Boron Nitride Fibers with Tailored Microstructures. Scientific Reports, 2017, 7, 3297.	3.3	26
84	Free-standing membranes made of activated boron nitride for efficient water cleaning. RSC Advances, 2015, 5, 71537-71543.	3.6	25
85	Four-dimensional vibrational spectroscopy for nanoscale mapping of phonon dispersion in BN nanotubes. Nature Communications, 2021, 12, 1179.	12.8	24
86	Visibleâ€toâ€Ultraviolet Light Conversion: Materials and Applications. Advanced Photonics Research, 2021, 2, 2000213.	3.6	24
87	Organic Fluorescent Dyes Supported on Activated Boron Nitride: A Promising Blue Light Excited Phosphors for High-Performance White Light-Emitting Diodes. Scientific Reports, 2015, 5, 8492.	3.3	21
88	Synthesis of Perovskite CsPbBr <sub>3</sub> Quantum Dots/Porous Boron Nitride Nanofiber Composites with Improved Stability and Their Reversible Optical Response to Ammonia. Inorganic Chemistry, 2020, 59, 1234-1241.	4.0	21
89	Europium (III) Organic Complexes in Porous Boron Nitride Microfibers: Efficient Hybrid Luminescent Material. Scientific Reports, 2016, 6, 34576.	3.3	19
90	Surface ligand engineering of CsPbBr3 perovskite nanowires for high-performance photodetectors. Journal of Colloid and Interface Science, 2022, 608, 2367-2376.	9.4	19

#	Article	IF	CITATIONS
91	Removal of Cr( <scp>iii</scp> )/Cr( <scp>vi</scp> ) from wastewater using defective porous boron nitride: a DFT study. Inorganic Chemistry Frontiers, 2018, 5, 1933-1940.	6.0	18
92	Solvothermal synthesis of Mn-doped CsPbCl <sub>3</sub> perovskite nanocrystals with tunable morphology and their size-dependent optical properties. RSC Advances, 2019, 9, 39315-39322.	3.6	16
93	Controllable synthesis of CsPbI <sub>3</sub> nanorods with tunable photoluminescence emission. RSC Advances, 2019, 9, 24928-24934.	3.6	15
94	Novel hierarchical RGO/MoS <sub>2</sub> /K-αMnO <sub>2</sub> composite architectures with enhanced broadband microwave absorption performance. Journal of Materials Chemistry C, 2019, 7, 13878-13886.	5.5	15
95	Isolated Au Atom Anchored on Porous Boron Nitride as a Promising Electrocatalyst for Oxygen Reduction Reaction (ORR): A DFT Study. Frontiers in Chemistry, 2019, 7, 674.	3.6	14
96	Anchoring of CsPbBr <sub>3</sub> perovskite quantum dots on BN nanostructures for enhanced efficiency and stability: a comparative study. Journal of Materials Chemistry C, 2021, 9, 842-850.	5.5	14
97	Hierarchically Porous Boron Nitride/HKUST-1 Hybrid Materials: Synthesis, CO <sub>2</sub> Adsorption Capacity, and CO <sub>2</sub> /N <sub>2</sub> and CO <sub>2</sub> /CH <sub>4</sub> Selectivity. Industrial & Engineering Chemistry Research, 2021, 60, 2463-2471.	3.7	14
98	Thin-walled B–C–N ternary microtubes: from synthesis to electrical, cathodoluminescence and field-emission properties. Journal of Materials Chemistry, 2012, 22, 8134.	6.7	11
99	Phosphorusâ€Modulationâ€Triggered Surface Disorder in Titanium Dioxide Nanocrystals Enables Exceptional Sodiumâ€Storage Performance. Angewandte Chemie, 2019, 131, 4062-4066.	2.0	11
100	Threeâ€Pronged Attack by Hybrid Nanoplatform Involving MXenes, Upconversion Nanoparticle and Aggregationâ€Induced Emission Photosensitizer for Potent Cancer Theranostics. Small Methods, 2022, 6, .	8.6	11
101	Graphene stirrer with designed movements: Targeting on environmental remediation and supercapacitor applications. Green Energy and Environment, 2018, 3, 86-96.	8.7	10
102	Design of Multifunctional Quinternary Metal-Halide Perovskite Compounds Based on Cation–Anion Co-Ordering. Chemistry of Materials, 2020, 32, 5949-5957.	6.7	10
103	Ultrahigh Aspect Ratio TiB Nanowhisker-Reinforced Titanium Matrix Composites as Lightweight and Low-Cost Replacements for Superalloys. ACS Applied Nano Materials, 2020, 3, 8208-8215.	5.0	9
104	Synthesis of boron nitride nanotubes using an oxygen and carbon dual-free precursor. RSC Advances, 2018, 8, 3989-3995.	3.6	8
105	Eco-green C, O co-doped porous BN adsorbent for aqueous solution with superior adsorption efficiency and selectivity. Chemosphere, 2022, 288, 132520.	8.2	8
106	Porous boron nitride nanofibers as effective nanofillers for poly(vinyl alcohol) composite hydrogels with excellent self-healing performances. Soft Matter, 2022, 18, 859-866.	2.7	8
107	Synthesis of Nanostructured Boron Nitride Aerogels by Rapid Pyrolysis of Melamine Diborate Aerogels via Induction Heating: From Composition Adjustment to Property Studies. ACS Applied Nano Materials, 2021, 4, 13788-13797.	5.0	8
108	Cobalt Supported on BN Catalyst with High Bâ $\in$ O Defects and Its Efficient Hydrodeoxygenation Performance of HMF to DMF**. ChemistrySelect, 2022, 7, .	1.5	7

#	Article	IF	CITATIONS
109	Self-sacrificed template synthesis of ribbon-like hexagonal boron nitride nano-architectures and their improvement on mechanical and thermal properties of PHA polymer. Scientific Reports, 2017, 7, 9006.	3.3	6
110	Ultrafine porous boron nitride nanofiberâ€ŧoughened WC composites. International Journal of Applied Ceramic Technology, 2020, 17, 941-948.	2.1	5
111	Highly Selective Hydrogenation of Phenol Catalyzed by Porous BN Supported Niâ^'Pd Catalysts. ChemistrySelect, 2021, 6, 5975-5982.	1.5	5
112	High yield synthesis and optical properties of MgF <sub>2</sub> nanowires with high aspect ratios. RSC Advances, 2016, 6, 29818-29822.	3.6	4
113	Facile Construction of a Solely-DNA-Based System for Targeted Delivery of Nucleic Acids. Nanomaterials, 2021, 11, 1967.	4.1	3
114	Delaminated Ti3C2Tx flake as an effective UV-protective material for living cells. Materials Letters, 2020, 260, 126972.	2.6	2
115	Theoretical Design of Inorganic Flexible Bulk Photovoltaic Materials. Journal of Physical Chemistry Letters, 2021, 12, 10182-10189.	4.6	1